AIP | Applied Physics Letters

Dynamically tunable plasmonically induced transparency in periodically patterned graphene nanostrips

Hua Cheng, Shuqi Chen, Ping Yu, Xiaoyang Duan, Boyang Xie et al.

Citation: Appl. Phys. Lett. **103**, 203112 (2013); doi: 10.1063/1.4831776
View online: http://dx.doi.org/10.1063/1.4831776
View Table of Contents: http://apl.aip.org/resource/1/APPLAB/v103/i20
Published by the AIP Publishing LLC.

Dynamically tunable plasmonically induced transparency in periodically patterned graphene nanostrips

Hua Cheng, Shuqi Chen,[a] Ping Yu, Xiaoyang Duan, Boyang Xie, and Jianguo Tian[a]
The Key Laboratory of Weak Light Nonlinear Photonics, Ministry of Education, School of Physics and Teda Applied Physics School, Nankai University, Tianjin 300071, China

(Received 11 July 2013; accepted 3 November 2013; published online 15 November 2013)

We present a dynamically wavelength tunable plasmonically induced transparency (PIT) planar device composed of periodically patterned graphene nanostrips for the mid-infrared region. The PIT effect can be achieved by a single layer of graphene nanostrips for a fixed Fermi energy. The PIT resonant wavelength can be dynamically tuned while maintaining PIT modulation strength, transmission peaks, and spectral line width by varying the Fermi energy of graphene without re-optimizing and re-fabricating the nanostructures. A three-level plasmonic system is demonstrated to well explain the formation mechanism of the wavelength tunable PIT in the graphene nanostrips. This work may offer a further step in the development of a compact tunable PIT device. © *2013 AIP Publishing LLC*. [http://dx.doi.org/10.1063/1.4831776]

Electromagnetically induced transparency (EIT), which is a quantum interference effect in laser-driven atomic systems, gives rise to a sharp transparency window within a broad absorption spectrum.[1] This phenomenon has found a variety of intriguing applications in quantum nonlinear optics, slow light, ultrafast switching, signal processing, and so on.[2,3] These applications require an abrupt change in dispersion over a narrow spectral range, where a sharp and pronounced spectral response is highly desired. Other than the classical analogues of EIT-like behavior in coupled resonators,[4] electric circuits,[5] and metallic nanostructures,[6] plasmonically induced transparency (PIT) based on metamaterial structures including cut wires,[7–9] split-ring resonators,[10–12] and coupled waveguide resonators[13] has attracted enormous research interest. PIT lays the foundation for the manipulation of light using metal nanostructures as an effective media with EIT-like optical properties, and can be realized in metamaterials via destructive interference between the superradiant and subradiant plasmonic modes or by breaking the symmetry of the metamaterial system. So far, most of the PIT effects observed in metamaterials have been realized at a fixed wavelength. In these cases, the PIT resonance has to be tuned to different wavebands by carefully reoptimizing and amplifying or reducing the geometric parameters of the structures. The ability to actively control the resonant constitutive elements of metamaterials will enable dynamic tunability of their optical response and will potentially expand the range of their applications even further.

Recently, many approaches to achieve dynamic tunability of plasmon energy have emerged which rely on integrating metamaterials with optically active materials such as nonlinear media,[14] semiconductors,[15] and liquid crystals.[16] As an alternative method, a single layer of continuous and structured graphene has been demonstrated to support surface plasmon polaritons[17,18] and can be a building material for metamaterials, which have attracted increasing attention for applications such as absorbers,[19] polarizers,[20] antennas,[21] and transformation optical devices.[22] Furthermore, the dielectric properties of graphene can be dynamically tuned by electrochemical potential via a chemical or electrostatic gating, magnetic field, or optical excitation.[23–25] This allows for the creation of surface plasmon based devices that can be effectively turned on and off or tuned to be active at different frequencies. Therefore, the combination of graphene and metamaterials is a promising approach to design a dynamically wavelength tunable PIT planar device, which remains an ongoing interest in the development of compact elements such as tunable sensors, switchers, and slow light devices.

In this Letter, we present a highly wavelength-tunable PIT device composed of graphene nanostrips for the mid-IR region. We demonstrate that PIT can be achieved using a single layer of graphene nanostructures. Wavelength-shift active control of the PIT resonance is realized by varying the Fermi energy of the graphene without reoptimizing and refabricating the nanostructures. Meanwhile, the three-level plasmonic system is demonstrated to well explain the formation mechanism of PIT in the graphene nanostrips, with analytical fitting results in good agreement with the numerical simulations.

The designed tunable PIT planar device based on graphene nanostrips is shown in Fig. 1. Optimization of the graphene structure was achieved using the finite element method (FEM) based software of COMSOL Multiphysics.[26] The three-dimensional simulations were performed for a single unit cell with x-polarized TEM beam normally incident in the z direction, and periodic boundary conditions in all x-z and y-z planes. The permittivity of the substrate is considered to be 2.1. The conductivity of graphene σ is computed within the local random phase approximation limit at the zero temperature[17]

$$\sigma(\omega) = \frac{e^2 E_F}{\pi\hbar^2}\frac{i}{\omega + i\tau^{-1}} + \frac{e^2}{4\hbar}\left[\theta(\hbar\omega - 2E_F) + \frac{i}{\pi}\left|\frac{\hbar\omega - 2E_F}{\hbar\omega + 2E_F}\right|\right]. \quad (1)$$

[a]Authors to whom correspondence should be addressed. Electronic addresses: schen@nankai.edu.cn and jjtian@nankai.edu.cn

The intrinsic relaxation time is expressed as $\tau = \mu E_F / e v_F^2$, where $v_F \approx c/300$ is the Fermi velocity and $\mu = 10000\ \mathrm{cm}^2/\mathrm{Vs}$ is the measured DC mobility.[27] The quantum confinement effects associated to the type of edges is ignored for nanostrip width above 20nm.[28]

To demonstrate the PIT effect in a single layer of graphene nanostrips, we numerically calculated its transmission spectra with different lateral displacement s in Figs. 2(a)–2(c) (blue balls), where the Fermi energy of graphene was fixed as 0.5 eV. An on-to-off PIT window modulation feature is apparent for the single layer of graphene nanostrips. A single resonance dip with transmission amplitude of 59% at 8.08 μm is observed in the absence of lateral displacement. The strong resonance demonstrates very efficient excitation of surface plasmons in the central graphene nanostrip, which corresponds to the collective oscillations of electrons across the length of the nanostrip. Actually, the x-polarized beam can also polarize the side graphene strips at the wavelength 5.2 μm. The resonant wavelengths are related to the width of the side graphene strip and the length of the central graphene strip when excited by the x-polarized beam. As the length of the central graphene strip is larger than the width of the side graphene strip, the two resonant wavelengths are far from each other. As the lateral displacement s is gradually increased from 3 nm to 12 nm, the transmission undergoes strong modulations, with transmission peaks emerging and increasing within the broad resonance profile. Finally, a PIT window with a transmission amplitude of 91% at 8.06 μm is achieved when the lateral displacement reaches 12 nm. We calculated the z-component distribution of the electric near-field in the x-y plane of the graphene nanostrips at the resonant wavelength with different lateral displacement s in Figs. 2(f)–2(j). Strong near-fields with opposite charges are concentrated near the central nanostrip edges in the absence of lateral displacement, which is consistent with the second edge mode in infinitely long graphene ribbons.[29] The origin of the resonance can be interpreted as the dipolar modes coupled to propagating light, which has strong field concentration at the central nanostrip ends. As the lateral displacement s is increased, the electric field distribution gradually shifts from the central nanostrip to the side nanostrips, as can be seen from Figs. 2(f)–2(j). This can be interpreted as due to the excitation of the second edge modes of the side graphene nanostrips via coupling with the dipolar modes of the central nanostrip. The antisymmetric dipole-dipole binding combination of the two graphene side nanostrips forms a nonradiative lateral quadrupole antenna. As the asymmetry of the nanostructure is increase, the antisymmetric charge oscillations and the coupling strength will further increase, corresponding to the transition from bright mode to dark mode. In our system, the central nanostrip serves as a broad-linewidth dipole antenna, which strongly couples with the incident light. A pair of two parallel nanostrips can act as a non-radiative quadrupole. The damping of the quadrupole antenna stems almost

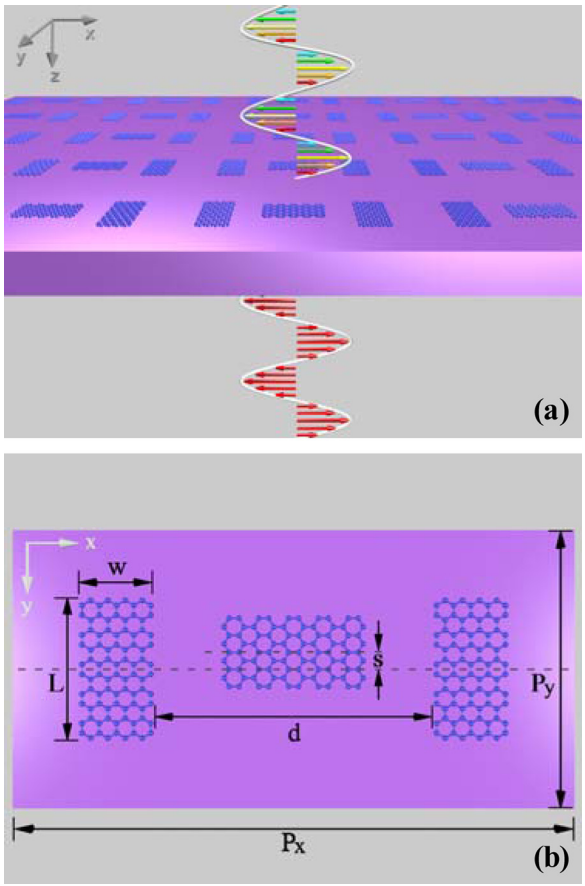

FIG. 1. (a) Schematic model of graphene nanostrips on a substrate and (b) unit cell structure of our design: strip length $L = 50$ nm, strip width $w = 25$ nm, side strip separation distance $d = 100$ nm, central strip lateral displacement s, periodicities $P_x = 200$ nm and $P_y = 100$ nm.

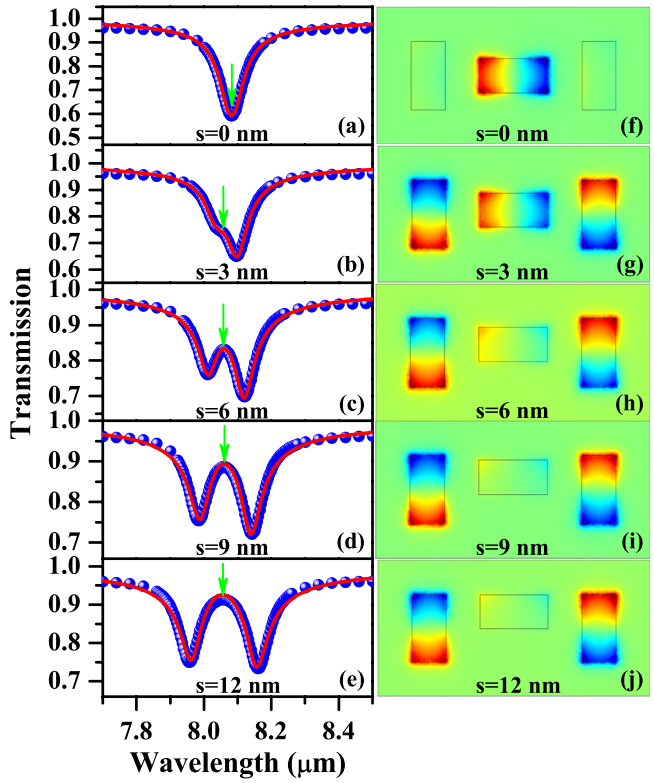

FIG. 2. Transmission spectra of numerical calculations by FEM (blue balls) and analytical fitting by three-level plasmonic system (solid red lines) of the PIT device for different lateral displacements s. The color maps represent the corresponding z component distributions of the electric field of the graphene nanostrips at the transmission peak wavelength of 8.06 μm. The cutting plane is 3 nm above the bottom of the graphene nanostrips. The Fermi energy of graphene is fixed as 0.5 eV. Green arrows indicate the positions of the PIT window.

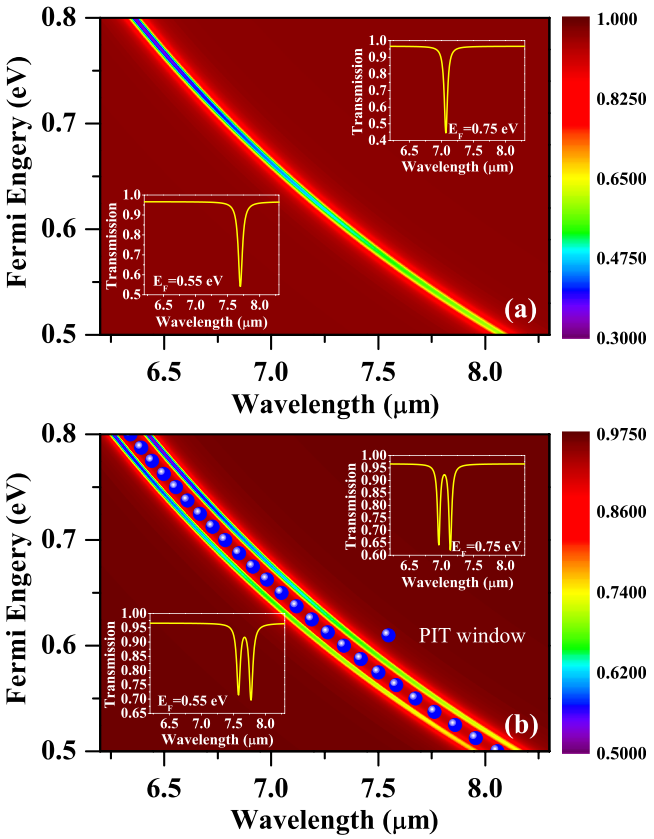

FIG. 3. Calculated transmission spectra as a function of Fermi energy and wavelength for lateral displacements of (a) $s = 0$ nm and (b) $s = 12$ nm. Insets show the transmission spectra for Fermi energies of 0.55 eV and 0.75 eV.

exclusively from intrinsic graphene losses. Therefore, we propose that the central nanostrip could serve as the bright mode in a PIT system.

To demonstrate the wavelength tunability of a PIT using the proposed graphene nanostrips, we graphed the transmission coefficient as a function of Fermi energy and wavelength for $s = 0$ nm and $s = 12$ nm, as shown in Fig. 3. The resonant strength of the graphene nanostrip is enhanced and blue shifted as the Fermi energy increases. To more clearly exhibit this behavior, we plot the transmission spectra for Fermi energies of 0.55 eV and 0.75 eV in the case of $s = 0$ nm and $s = 12$ nm, respectively, in the insets of Fig. 3. The resonant wavelengths are at 7.7 μm and 7.1 μm for Fermi energies of 0.55 eV and 0.75 eV, respectively. This behavior can be interpreted through the resonance condition. The wave vector of surface plasmons along the graphene nanostrip satisfies $k_{spp} \propto 1/L$ and $k_{spp} = \hbar\omega_r{}^2/(2\alpha_0 E_F c) = \frac{2\pi^2\hbar c}{\alpha_0 E_F \lambda_r^2}$,[17] where L represents the length of the graphene nanostrip, $\alpha_0 = e^2/(\hbar c)$ is the fine structure constant, and λ_r is the resonant wavelength. Thus, the resonant wavelength can be written as $\lambda_r \propto \sqrt{2\pi^2\hbar c L/(\alpha_0 E_F)}$. Hence, the resonance and PIT wavelengths can be tuned by varying the Fermi energy while fixing the geometrical parameters, indicating that graphene nanostructures are more active for the PIT effect than metallic ones, and thus may find applications in compact elements such as tunable sensors, switchers, and slow light devices.

The physics of the PIT can be better understood if we examine the analogy between our system and atomic EIT systems. To explore the physical origin of the wavelength-tunable PIT behavior, the widely used three-level plasmonic system is adapted to analyze the near field interaction between the graphene nanostrips in a PIT unit cell. This model involves a radiative plasmonic state $|1\rangle = \tilde{A}_1(\omega)e^{i\omega t}$ (bright mode) and a dark plasmonic state $|2\rangle = \tilde{A}_2(\omega)e^{i\omega t}$ (dark mode), which have resonant frequencies ω_{01}, ω_{02} and damping factors γ_1, γ_2, respectively. A three-level plasmonic system is formed by two states of coupled meta-atoms and a continuum state (ground state $|0\rangle$). $|0\rangle - |1\rangle$ defines a dipole-allowed transition, which is analogous to the mode excited in the dipole antenna in our system. $|0\rangle - |2\rangle$ defines a dipole-forbidden transition, which is analogous to the mode that can be excited in the quadrupole antenna when structural asymmetry is present. The transition between states $|1\rangle$ and $|2\rangle$ is related to the coupling between the dipole and quadrupole antennas. Therefore, the two possible pathways of $|0\rangle - |1\rangle$ and $|0\rangle - |1\rangle - |2\rangle - |1\rangle$ interfere destructively, reducing losses and enhancing transmittance. The interference can be analytically described by the coupled Lorentz oscillator model as

$$\begin{bmatrix} \omega - \omega_{01} + i\gamma_1 & \kappa \\ \kappa & \omega - \omega_{02} + i\gamma_2 \end{bmatrix} \begin{bmatrix} \tilde{A}_1 \\ \tilde{A}_2 \end{bmatrix} = -\begin{bmatrix} g\tilde{E}_0 \\ 0 \end{bmatrix}, \quad (2)$$

where κ is the coupling coefficient between $|1\rangle$ and $|2\rangle$, and g is a geometric parameter indicating the coupling strength of the bright mode with incident electromagnetic field $\tilde{E}_0 e^{i\omega t}$. The complex amplitude of the bright mode $\tilde{A}_1$ is directly proportional to the polarizability of the PIT system. Thus, the transmission can be obtained by $T(\omega) = 1 - |\tilde{A}_1/\tilde{E}_0|^2$. The analytical fitting of Eq. (2) to the FEM numerical transmission spectra under different lateral displacements is shown in Fig. 2, and exhibits very good agreement with the numerical calculations, confirming the validity of our designed graphene based PIT device. The fitting parameters with different lateral displacements and Fermi energies are plotted in Fig. 4. When the Fermi energy is fixed (see Fig. 4(a)), the coupling coefficient κ is approximately proportional to the lateral displacement s, indicating that the coupling strength between the dipole and quadrupole antennas successively increased with structural asymmetry. The damping rate of the bright mode γ_1 reduces markedly, by two orders of magnitude, as the lateral displacement s increases from 0 to 6 nm, and then keeps roughly constant with further increase in s. The damping rate of the graphene bright mode includes two components: one for the non-radiative damping due to the intrinsic graphene loss, and another for radiative damping. From Figs. 2(f)–2(h), we can see that the distribution of electric field in the central graphene strip (bright mode) decreases quickly as the lateral displacement s increases from 0 to 6 nm. Therefore, the non-radiative damping due to the intrinsic graphene loss significantly decreases with increasing lateral displacement s. The damping rate is gradually dominated by the radiative damping, which is approximately two orders smaller than the non-radiative damping in graphene.[19] Meanwhile, the damping rate of the dark mode γ_2 is two orders larger than that of the bright mode γ_1 when the lateral displacement is larger than 6 nm. In this case, γ_2 is dominated by the non-radiative damping factor, limited mainly by the intrinsic graphene loss.

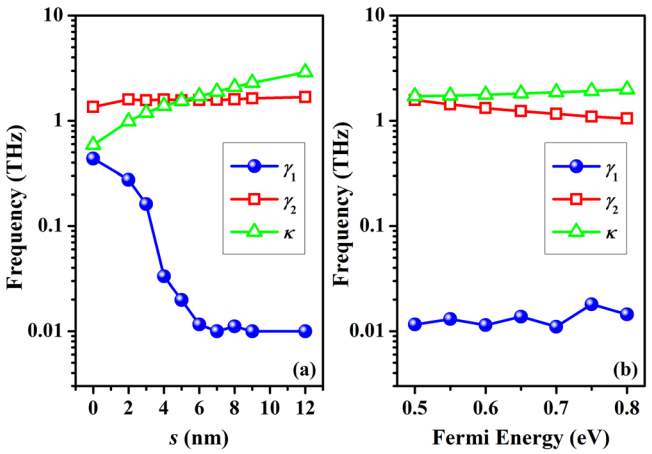

FIG. 4. Extracted numerical coupling and damping parameters as a function of (a) lateral displacement at fixed Fermi energy of $E_F = 0.5$ eV and (b) Fermi energy at fixed lateral displacement of $s = 6$ nm. Values of γ_1, γ_2, and κ were extracted by fitting the numerical transmission spectra.

In Fig. 4(b), the radiative damping γ_1 has a small increasing trend with Fermi energy. However, the damping rates γ_1, γ_2 and the coupling strength κ do not vary significantly with increasing Fermi energy when the lateral displacement is fixed. This implies that variation in Fermi energy hardly affects the modulation strength, transmission peaks, and the spectral linewidth of the PIT effect of the graphene nanostrips, merely tuning the PIT to shorter or longer wavelengths. These features can also be seen from Fig. 3(b). Such quantitative results confirm our expectations about an ideal wavelength-tunable PIT device based on graphene nanostrips.

In conclusion, we have proposed a dynamically wavelength tunable PIT planar device for the mid-infrared region based on graphene nanostrips. The PIT effect can be achieved using a single layer of graphene nanostrips for a fixed Fermi energy. Moreover, by varying the Fermi energy of the graphene, the wavelength of the PIT resonance can be dynamically tuned without the need to re-optimize or re-fabricate the nanostructures while maintaining PIT modulation strength, transmission peaks, and spectra linewidth. This makes graphene PIT device more useful than metallic PIT devices. We believe that this method of actively tuning the wavelength of PIT may open up avenues for the development of compact elements such as tunable sensors, switchers and slow light devices.

This work was supported by the Chinese National Key Basic Research Special Fund (No. 2011CB922003), the National Basic Research Program (973 Program) of China (No. 2012CB921900), the Natural Science Foundation of China (Nos. 11304163, 61378006, and 61008002), the Program for New Century Excellent Talents in University (No. NCET-13-0294), the Natural Science Foundation of Tianjin (No. 13JCQNJC01900), the Specialized Research Fund for the Doctoral Program of Higher Education (Nos. 20120031120032 and 20100031120005), and the 111 project (No. B07013).

[1]S. E. Harris, Phys. Today **50**(7), 36 (1997).
[2]T. F. Krauss, Nat. Photonics **2**, 448 (2008).
[3]M. Fleischhauer, A. Imamoglu, and J. P. Marangos, Rev. Mod. Phys. **77**, 633 (2005).
[4]X. Yang, M. Yu, D. Kwong, and C. W. Wong, Phys. Rev. Lett. **102**, 173902 (2009).
[5]C. L. Garrido Alzar, M. A. G. Martinez, and P. Nussenzveig, Am. J. Phys. **70**, 37 (2002).
[6]V. Yannopapas, E. Paspalakis, and N. V. Vitanov, Phys. Rev. B **80**, 035104 (2009).
[7]S. Zhang, D. A. Genov, Y. Wang, M. Liu, and X. Zhang, Phys. Rev. Lett. **101**, 047401 (2008).
[8]N. Liu, L. Langguth, T. Weiss, J. Kästel, M. Fleischhauer, T. Pfau, and H. Giessen, Nature Mater. **8**, 758 (2009).
[9]X. Duan, S. Chen, H. Yang, H. Cheng, J. Li, W. Liu, C. Gu, and J. Tian, Appl. Phys. Lett. **101**, 143105 (2012).
[10]J. Gu, R. Singh, X. Liu, X. Zhang, Y. Ma, S. Zhang, S. A. Maier, Z. Tian, A. K. Azad, H. Chen, A. J. Taylor, J. Han, and W. Zhang, Nature Commun. **3**, 1151 (2012).
[11]Z. Li, Y. Ma, R. Huang, R. Singh, J. Gu, Z. Tian, J. Han, and W. Zhang, Opt. Express **19**, 8912 (2011).
[12]X. Liu, J. Gu, R. Singh, Y. Ma, J. Zhu, Z. Tian, M. He, J. Han, and W. Zhang, Appl. Phys. Lett. **100**, 131101 (2012).
[13]H. Lu, X. Liu, G. Wang, and D. Mao, Nanotechnology **23**, 444003 (2012).
[14]A. A. Zharov, I. V. Shadrivov, and Y. S. Kivshar, Phys. Rev. Lett. **91**, 037401 (2003).
[15]N. Shen, M. Massaouti, M. Gokkavas, J. Manceau, E. Ozbay, M. Kafesaki, T. Koschny, S. Tzortzakis, and C. M. Soukoulis, Phys. Rev. Lett. **106**, 037403 (2011).
[16]S. Khatua, W. Chang, P. Swanglap, J. Olson, and S. Link, Nano Lett. **11**, 3797 (2011).
[17]F. H. L. Koppens, D. E. Chang, and F. Javier García de Abajo, Nano Lett. **11**, 3370 (2011).
[18]L. Ju, B. Geng, J. Horng, C. Girit, M. Martin, Z. Hao, H. A. Bechtel, X. Liang, A. Zettl, Y. R. Shen, and F. Wang, Nat. Nanotechnol. **6**, 630 (2011).
[19]S. Thongrattanasiri, F. H. L. Koppens, and F. Javier García de Abajo, Phys. Rev. Lett. **108**, 047401 (2012).
[20]A. Fallahi and J. Perruisseau-Carrier, Phys. Rev. B **86**, 195408 (2012).
[21]Z. Fang, S. Thongrattanasiri, A. Schlather, Z. Liu, L. Ma, Y. Wang, P. M. Ajayan, P. Nordlander, N. J. Halas, and F. Javier García de Abajo, ACS Nano **7**, 2388 (2013).
[22]A. Vakil and N. Engheta, Science **332**, 1291 (2011).
[23]K. I. Bolotin, K. J. Sikes, Z. Jiang, M. Klima, G. Fudenberg, J. Hone, P. Kim, and H. L. Stormer, Solid State Commun. **146**, 351 (2008).
[24]A. K. Geim, Science **324**, 1530 (2009).
[25]K. S. Novoselov, V. I. Fal'ko, L. Colombo, P. R. Gellert, M. G. Schwab, and K. Kim, Nature **490**, 192 (2012).
[26]COMSOL Multiphysics User's Guide, version 3.5, Comsol AB, Burlington, MA, 2008.
[27]K. S. Novoselov, A. K. Geim, S. V. Morozov, D. Jiang, Y. Zhang, S. V. Dubonos, I. V. Grigorieva, and A. A. Firsov, Science **306**, 666 (2004).
[28]S. Thongrattanasiri, A. Manjavacas, and F. Javier. García de Abajo, ACS Nano **6**, 1766 (2012).
[29]J. Christensen, A. Manjavacas, S. Thongrattanasiri, F. H. H. Koppens, and F. Javier García de Abajo, ACS Nano **6**, 431 (2012).